Oxidation and Hydrolysis of Lactic Acid in Near-Critical Water

Lixiong Li,[†] Juan R. Portela,[‡] David Vallejo,[†,§] and Earnest F. Gloyna*,[†]

Environmental and Water Resources Engineering Program, Civil Engineering Department, The University of Texas at Austin, Austin, Texas 78712, and Departmento de Ingenieria Quimica, Universidad de Cadiz, 11510 Puerto Real, Cadiz, Spain

Hydrothermal reactions (oxidation and hydrolysis) involving lactic acid (LA) were studied at temperatures ranging from 300 to 400 °C and a nominal pressure of 27.6 MPa. Kinetic models were developed with respect to concentrations of LA and total organic carbon (TOC), respectively. The best-fit model for LA oxidation with 95% confidence limits is $-d[LA]/dt = 10^{18.7\pm4.2} \times \exp(-226 \pm 46.6 \text{ kJ/mol}/RT)[LA]^{0.88\pm0.11}[O_2]^{0.16\pm0.19}$. Similarly, the best-fit TOC model for lactic acid oxidation is $-d[TOC]/dt = 10^{4.3\pm2.5} \exp(-68.4 \pm 27.2 \text{ kJ/mol}/RT)[TOC]^{0.62\pm0.33}[O_2]^{0.36\pm0.26}$. The best-fit TOC model for lactic acid hydrolysis is $-d[TOC]/dt = 10^{8.4\pm2.1} \exp(-125 \pm 26.7 \text{ kJ/mol}/RT)[TOC]$. On the basis of identified liquid and gaseous products, pathways for hydrothermal reactions involving lactic acid were proposed. Acetic acid and acetaldehyde were confirmed as the major liquid intermediates for oxidation and hydrolysis reactions, respectively. Carbon monoxide and methane were identified as the major gaseous byproducts from these reactions. These results demonstrated the potential of completely oxidizing, as well as converting, lactic acid into other organic products, in high-temperature water.

Introduction

There is a growing interest in hydrothermal reactions involving organic and inorganic compounds. High-temperature water, particularly at conditions near the vapor−liquid critical point of water (374.2 °C and 22.1 MPa), can be an efficient and unique reaction medium for gasification,[1,2] hydrolysis,[3,4] oxidation,[5−9] dehydration,[10,11] thermal decomposition,[12,13] and acid−base reactions.[14,15] Supercritical water (SCW) is an excellent solvent for organic compounds and gases such as oxygen. Also, mixing processes are enhanced as a result of the low viscosity and high diffusivity of water in the critical region. The high heat capacity of water makes it an excellent heat carrier and heat-transfer medium.

Hydrothermal oxidation (HTO) is a typical example of the potential use of high-temperature water media for waste treatment and chemical processing. HTO processes can be operated at conditions below or above the critical point of water. The former, known as wet air oxidation (WAO), is typically operated at temperatures and pressures, respectively, ranging from 200 to 330 °C, and from 2 to 20 MPa.[16] The latter, often referred to as supercritical water oxidation (SCWO), is carried out at temperatures and pressures, respectively, ranging from 400 to 650 °C, and from 25 to 35 MPa.[17] For SCWO, organic destruction efficiencies of greater than 99.9% can be generally achieved within 1 min of reactor residence times.

Recently, integrated HTO treatment and processing concepts have been explored through studies involving the conversion of wastes into useful products[18] and product separation/recovery.[19] To support engineering designs and process development for waste conversion and product recovery applications, it is important to understand reaction pathways and establish kinetic models and databases. Several key reaction intermediates have been identified by previous studies involving the HTO treatment of organic wastes. Acetic acid is generally considered one of the most refractory organic intermediates.[20,21] For this reason, reaction kinetics involving acetic acid oxidation and hydrolysis in subcritical and supercritical water has been extensively studied.[21−25] Other short-chain carboxylic acids that have been studied under HTO conditions include formic acid,[26−28] oxalic acid,[28,29] propionic acid,[27] lactic acid,[18] butyric acid,[27] and tartaric acid.[28] Global kinetic models are available for the oxidation of formic acid[26,30,31] and oxalic acid[32] in subcritical and supercritical water.

For waste treatment purposes, the decomposition of lactic acid in high-temperature water is not a rate-limiting step as compared to that of acetic acid. However, lactic acid is a product derived from biomass via fermentation or other chemical processes, and it can be an important intermediate for synthesizing other organic compounds.[33] Recent studies involving reactions of lactic acid in and/or with high-temperature water include the conversion of lactic acid to acrylic acid via dehydration,[10,34] and to 2,3-pentanedione and acrylic acid over various catalysts.[35,36] For chemical-processing purposes, it is also important to study hydrolysis and partial oxidation of lactic acid in high-temperature water. Therefore, the purpose of this study was to develop kinetic correlations for hydrolysis and oxidation of lactic acid and identify key reaction pathways associated with reactions of lactic acid in subcritical and supercritical water.

Experimental Apparatus and Procedure

A laboratory-scale, continuous-flow reactor system was used in this study. As shown in Figure 1, the major components of this system included (1) two air-driven, high-pressure feed pumps (Williams Model CP205-W300B316TG), (2) a coiled preheater, (3) a coiled

* To whom correspondence should be addressed.
† The University of Texas at Austin.
‡ Universidad de Cadiz.
§ Graduate Student, UT SCWO Projects. Current address: Burns & McDonnell WCI, 9400 Ward Parkway, Kansas City, MO 64114.
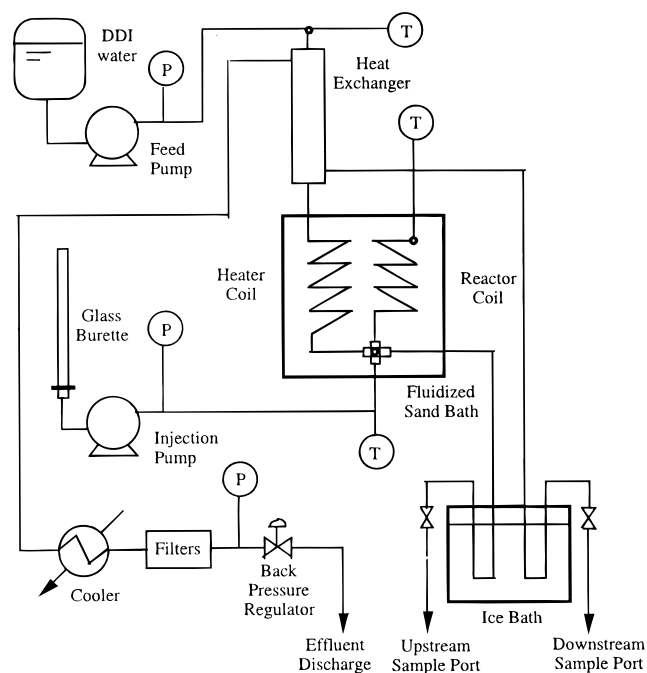
Figure 1. Schematic flow diagram of the continuous-flow reactor system.

reactor, (4) a heat exchanger, (5) a filter assembly, (6) a back-pressure regulator, and (7) thermocouples and pressure indicators at various locations. All wetted parts, from the pumps to the back-pressure regulator, were made of Stainless Steel 316. Both the preheater and the reactor were made of 0.318-cm o.d. (0.140 cm i.d.) Stainless Steel 316 tubing. The lengths of the preheater (280 cm) and reactor (400 cm) were selected based on heat-transfer and reaction time requirements, respectively. Both of these tubings were coiled and submerged in a fluidized sand bath (Techne Model SBL-2). Thermocouples (Omega Type K P/N KQIN) were installed at the reactor inlet (the reactor upstream) and at the reactor outlet (the reactor downstream). Typically, the difference between the upstream and downstream fluid temperatures was less than 4 °C. The average of these two temperatures was used as the reaction temperature. Upon exiting the reactor, the effluent was cooled via the feed heat exchanger and the chilled water cooler. Then, the process pressure was reduced to ambient conditions via the back-pressure regulator (Whitey SS-31RS4).

Sample ports were installed at the reactor inlet and outlet, respectively. The sample lines were made of 0.159-cm o.d. (0.0529-cm i.d.) Stainless Steel 316 tubing and were submerged in an ice bath. The sampling was controlled by the valve (HIP tapered stem shut-off valve) at the end of each sample line. A 60-cm³ granulated polyethylene syringe was connected at the downstream of each shut-off valve. This procedure allowed both gaseous and liquid effluents to be collected within the sample syringe and the volumetric ratios of gas and liquid effluents to be obtained. During sampling, the flow rate was maintained relatively small as compared to the total fluid flow rate passing through the reactor.

To start an experiment, the fluidized sand bath was first heated to the desired temperature. Both the feed and injection pumps were started using distilled and deionized (DDI) water as feed. After the pump flow rates, reactor pressure, and temperature stabilized, the feed and injection pump inlets were switched to the feed

solutions. Typically, 30−60 min were used to stabilize the reactor system. A dilute hydrogen peroxide aqueous solution (the concentration of H_2O_2 varied according to the lactic acid concentration and [O₂]/[LA] ratio) was introduced by the feed pump and was heated to the reaction temperature as it passed through the heat exchanger and the preheater.

At the preheater−reactor junction, the lactic acid solution was introduced by the injection pump. To avoid excess cooling of the hot oxidant stream by the cold lactic acid solution, the flow rate of the cold stream was maintained between 6 and 14 wt % of that of the hot stream. Typically, the reactor system was allowed to stabilize for about 15 min after the feed solutions were introduced. At each test condition, samples were collected at the reactor downstream sample port. To collect reactor effluent samples, the sample line was first purged for about 3 min, and the back-pressure regulator was adjusted to minimize pressure fluctuation.

Flow rates for the feed and injection streams ranged from 10 to 30 cm³/min and from 2 to 10 cm³/min, respectively. The flow rates were measured repeatedly using granulated cylinders and a stopwatch until a steady-state condition was reached. The duration of each flow measurement was typically about 2 min. The accuracy of the volumetric flow measurement was within ±3%. Pressure was fixed at 27.6 ± 0.2 MPa. Temperatures ranged from 300 to 400 °C with variations of less than ±1 °C. Reactor residence times were calculated from the density of water at the experimental conditions, reactor volume, and the total feed flow rate (feed stream plus injection stream). On the basis of these uncertainties of the individual parameters, the compounded errors in the calculated reactor residence times were believed to be less than ±5% of the reported values.

Materials and Analytical Methods

D−L-Lactic acid (Aldrich, 85% aqueous solution) and hydrogen peroxide (35% aqueous solution) were used. Dilutions of these stock solutions for preparing feed solutions of required concentrations were made using DDI water.

An ion chromatograph (Dionex System 14), equipped with a conductivity detector and an anion column (Dionex AS-1), was used to quantify acetic, lactic, formic, and glycolic acids. Sodium borate ($Na_2B_4O_7$) solution was used as the eluent. The ion chromatograph was calibrated daily prior to and during the sample analysis. The calibration was based on at least five different concentrations of the standard solutions. Since elution peaks of acetic and lactic acids were relatively close, an enzymatic colorimetric method (Sigma 735-10) was used to quantify lactic acid and confirm the ion chromatograph separation results.

Gaseous effluent samples were analyzed using two gas chromatographs (GC). One (Fisher-Hamilton Model 29) was used to quantify carbon dioxide and the other (Hewlett-Packard Model 5750) was used to establish the concentrations of carbon monoxide, oxygen, nitrogen, and methane. The Fisher-Hamilton GC was equipped with a 0.3-m long and 6.35-mm o.d. silica gel column and a thermal conductivity detector. This GC was operated isothermally at 25 °C with a helium carrier flow rate of 20 mL/min. The signal output was recorded using an integrator (Hewlett-Packard Model 3392A). The second GC employed a 3.05-m long × 3.175-mm o.d.

Table 1. Test Conditions, Reaction Rate Data, and Gaseous Byproducts Derived from Hydrothermal Oxidation of Lactic Acid[a]

temp (°C)	[LA] (mg/L)	$[O_2]_0/[LA]_0$ (molar)	stoich. O_2 (%)	time (s)	N_{Re}	LA conv. (%)	TOC conv. (%)	O_2 (%)	N_2 (%)	CH_4 (%)	CO (%)	CO_2 (%)	carbon closure (%)
300	999.2	6	201	8.1	5584	18.8	46.3	63.4	2.23	BDL	0.17	n/s	
300	971.9	6	206	11.5	3942	18.2	31.4	63.5	1.24	BDL	0.21	n/s	
300	1042	6	191	15.3	2956	24.6	43.1	67.2	2.24	0.07	0.1	n/s	
315	559.5	3	88	6.9	6621	37.5	41.2	77.8	6.24	BDL	0.7	3.6	78.1
315	538.6	3	92	14.1	3258	34.6	41.6	79.6	6.18	BDL	0.6	2.7	74.4
315	513.8	3	98	44.1	1045	81.4	57.8	72.9	n/a	n/a	3.3	7.8	90.8
315	581.6	6	168	7.0	6534	65.4	54	77.2	n/a	n/a	0.9	6	82.3
315	532.9	6	185	14	3311	58	42.4	81.4	5.02	BDL	0.4	2.6	75.0
315	522.1	6	192	42.7	6273	83.5	59.5	78.4	4.51	0.06	1.8	6.6	86.5
315	989.6	6	202	7.4	1742	59.9	57.4	87.1	0.47	0.6	0.2	3.4	
315	935.8	6	215	26.5	1045	71.1	53.9	84.7	n/a	n/a	0.6	3.3	
315	954.7	6	210	44.1	1045	87.7	67.7	81.6	0.36	1.53	0.1	4.4	
325	514.9	3	96	6.8	6902	50.1	41.7	77.4	6.16	BDL	1.0	6.0	93.3
325	522.1	3	95	13.7	3396	44.3	44.2	75.7	6.51	BDL	1.3	4.5	83.6
325	493.3	3	103	42.8	1090	99.9	64.2	68.2	6.3	0.11	5.4	10.7	103
325	989.6	6	202	7.1	6538	42.9	40.7	87.1	2.57	BDL	0.7	4.3	
325	984.8	6	203	16.1	2906	82.7	59.4	84.5	2	BDL	1.2	5.1	
325	972.7	6	206	32.1	1453	88.6	58.2	80.8	2.16	0.12	2.5	11.5	
325	1937	9	311	6.6	6902	94.1	64.6	75.8	1.24	BDL	1.2	9.5	83.2
325	2076	9	287	13	3632	90.5	62.5	75.9	1.24	0.05	1.3	9.2	80.6
335	505.8	3	98	6.5	7213	58.2	46.7	74.2	6.16	0.05	2.3	6.6	94.2
335	1060	1	31	6.5	7213	60.1	48.1	31	10.3	0.22	9.2	n/s	
335	1059	1	31	12.9	3607	76.9	57.9	41	11.7	0.3	20.3	n/s	
335	1010	6	199	5.8	7403	62.5	55.4	71.2	2.89	BDL	1.6	7.9	
335	1005	6	199	8.3	5695	91	60.9	n/a	n/a	n/a	n/a	n/a	
335	996.5	6	200	11.3	4176	93.1	68.2	83.3	2.35	1.43	0.2	7.3	
335	1988	6	201	6.5	7213	93.8	65	70.1	1.77	0.05	2.3	13.5	87.2
335	2049	6	194	20.5	2297	99.9	68.8	64.6	2	0.11	2.7	14.2	81.9
335	1940	6	207	39.5	1177	>99.9	71.2	67.6	2.07	0.16	2.7	12.7	75.0
350	1010	1	33	6.2	7669	85.7	66.7	16.1	12.26	1.39	41.2	n/s	
350	989.7	1	34	12.4	3886	>99.9	69	1.8	11.9	2.51	48.9	n/s	
350	2007	3	100	6.1	7853	>99.9	71.6	51.6	3.63	0.12	7.6	27.6	97.0
350	2027	3	98	37.1	1288	>99.9	72.3	51.9	3.9	0.29	7.9	24.6	88.3
365	2028	3	99	5.7	8534	>99.9	78.3	46	3.32	0.3	11.4	29.6	96.1
365	2046	3	97	34.1	1415	>99.9	80.1	46.4	3.58	0.38	11	27.1	88.2
380	1018	6	202	5.8	8304	>99.9	81.2	49.2	3.28	0.15	6.4	n/a	
380	1025	6	194	7.8	6228	>99.9	80.6	59.1	3.48	0.48	8.1	n/a	
380	853	6	202	10.4	4671	>99.9	84.3	56.5	2.66	0.12	5.7	n/a	
400	908	6	221	3.4	11540	>99.9	88	50	1.67	0.13	7.4	n/a	

[a] n/s, not enough sample to complete the analysis; n/a, not available; BDL, below detection limit.

molecular sieve (Supelco 5A) column and a thermal conductivity detector. The column was maintained isothermally at 69 °C. The signal output was recorded using an integrator (Spectra-Physics Model 4290). Both chromatographs were calibrated using 1% and 15% v/v gas standards.

Total organic carbon (TOC) contents of liquid effluent samples were monitored. The analysis was performed using a TOC analyzer (Shimadzu Model 5050) and following Standard Method 5310C. Multiple injections (two to four times) were made for all samples to establish the reproducibility of the results.

Results and Discussion

A total of 39 oxidation experiments were conducted under various temperature, lactic acid concentration, and oxygen concentration conditions, as shown in Table 1. Lactic acid and TOC concentrations at the reactor inlet were calculated from the feedstock concentrations and pump flow rates. Lactic acid and TOC concentrations at the reactor outlet were analytically determined. Table 1 also shows lactic acid and TOC conversions derived from the measured concentration data. When these conversions were correlated with the reactor residence time, kinetic models for lactic acid reactions in hydrothermal environments were obtained.

Reaction Kinetics. Kinetic models were obtained for the HTO of lactic acid based on the power-law rate expression shown in eq 1:

$$-\frac{d[LA]}{dt} = k[LA]^m[O_2]^n \tag{1}$$

and

$$k = A \exp\left(-\frac{E_a}{RT}\right) \tag{2}$$

where t is time (s), [LA] and $[O_2]$ are concentrations of lactic acid and oxygen (mole/L), m and n are reaction orders with respect to lactic acid and oxygen, respectively, k is the reaction rate constant, A is the pre-exponential factor, E_a is the activation energy (J/mol), R is the universal gas constant (8.314 J/mol K), and T is the temperature (K). A similar rate expression for TOC associated with the HTO of lactic acid is given below:

$$-\frac{d[TOC]}{dt} = k[TOC]^m[O_2]^n \tag{3}$$

In these models, the oxygen concentration, $[O_2]$, is calculated from the complete decomposition of H_2O_2 in

Table 2. Kinetic Parameters for Hydrothermal Oxidation of Selected Carboxylic Acids

organic compd	m	n	A ([mol/L]$^{1-m-n}$/s)	E_a (kJ/mol)	temp (°C)	ref
			Best-Fit Models			
lactic acid[a]	0.88	0.16	5.49×10^{18}	226	315–360	this work
(TOC) (LA)[a]	0.62	0.36	2.18×10^4	68.4	315–360	this work
formic acid	1.33	0.46	3.10×10^9	144	190–313	26
oxalic acid	1	0.31	6.83×10^8	134	227–300	42
acetic acid	1	0.37	5.60×10^{10}	168	270–320	26
acetic acid	0.72	0.27	7.94×10^9	168	425–600	25
acetic acid[a]	1.01	0.16	3.47×10^{11}	180	415–525	22
			Pseudo-First-Order Models			
lactic acid[a]	1	0	1.52×10^{19}	230	315–360	this work
(TOC) (LA)[a]	1	0	2.23×10^3	54.4	315–360	this work
acetic acid[a]	1	0	9.12×10^{10}	167	415–525	22
acetic acid	1	0	2.55×10^{11}	173	338–445	30
acetic acid	1	0	7.91×10^{10}	174	385–440	19
acetic acid	1	0	1.26×10^{11}	183	425–600	25
TOC (AA)	1	0	4.40×10^{12}	182	270–320	26

[a] Hydrogen peroxide was used as the oxidant.

the feed stream. Retention times of the hydrogen peroxide feed in the preheater were estimated to be 12 and 7.3 s to reach 300 and 380 °C, respectively. On the basis of published kinetic data for the thermal decomposition of H_2O_2 in high-temperature water greater than 97% of H_2O_2 would be decomposed under these conditions.[37] Therefore, a small fraction of H_2O_2 could have survived as the feed entering the reactor inlet. However, had O_2 been used as the oxidant, H_2O_2 would have been present in the HTO environment, as indicated by analyzing known oxidation mechanisms[20] and as has been experimentally verified using selected alcohols.[38] Since H_2O_2 is more readily able to generate OH radicals than O_2 is, the presence of a small amount of H_2O_2 at the reactor inlet would enhance the rate of hydrogen abstraction.[22,39] Therefore, the selectivity of lactic acid decomposition among various reaction pathways may be affected.

On the basis of the oxidation stoichiometry, 3 mol of oxygen are required for complete oxidation of 1 mol of lactic acid. The oxidation tests were conducted at initial oxygen to lactic acid molar ratios of 1, 3, 6, or 9. However, only a few tests were conducted at substoichiometric oxygen concentrations (i.e., [O_2]/[LA] molar ratio = 1). Because many reaction intermediates resulting from incomplete oxidation of lactic acid were identified, the theoretical stoichiometric ratio for lactic acid oxidation to CO_2 and H_2O could not be used. To calculate the oxygen concentration at any given time, the oxygen concentration was correlated to TOC reduction. A few data points, corresponding to lactic acid conversions near zero (300 °C) or near 100% (360–400 °C), were excluded from data regression for the lactic acid kinetic model.

The experimental conditions were selected to meet plug-flow criteria.[40] The plug-flow reactor assumption held even at the lowest Reynolds number of 1080 corresponding to 315 °C and 6.2 cm³/min since surface reactions in this reaction system were negligible. Estimated kinetic parameters for both lactic acid and TOC models are given in Table 2. In both cases, the overall reaction (i.e., $m + n$) appears to be approximately first-order. Therefore, pseudo-first-order models with respect to lactic acid concentration and TOC concentration, respectively, are also presented in Table 2. For models involving lactic acid concentration, the activation energy changed slightly (<2%) when the best-fit model was replaced by the pseudo-first-order model. The pseudo-first-order Arrhenius plot for the HTO of lactic acid is
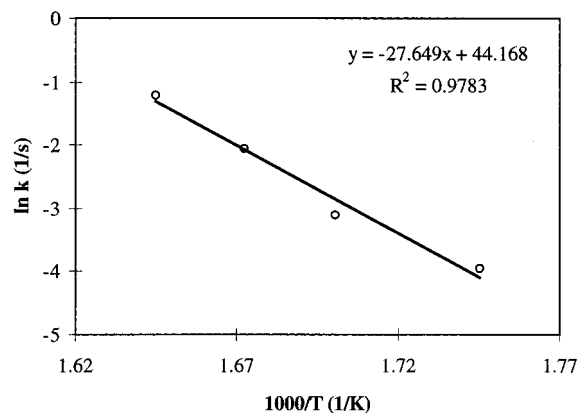
Figure 2. Arrhenius plot for HTO of lactic acid (pseudo-first-order model).
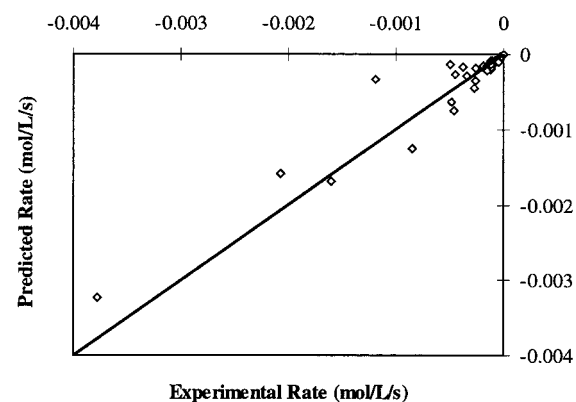
Figure 3. Lactic acid oxidation rate: predicted vs observed values.

shown in Figure 2. Similarly, as shown in Figure 3, the predicted lactic acid oxidation rate compares favorably with the experimental data. Only three tests at 300 °C displayed a statistically significant discrepancy in lactic acid and TOC conversions, that is, the lactic acid conversion was lower than that of TOC. However, subtracting these data from the regression did not show a significant effect on the modeling results. In this case, the error could be derived from some unexpected interference in the IC measurement.

The activation energy associated with the HTO of lactic acid (226 ± 46.6 kJ/mol) is higher than that of acetic acid (168–180 kJ/mol). Such high activation energies have also been reported for other organic
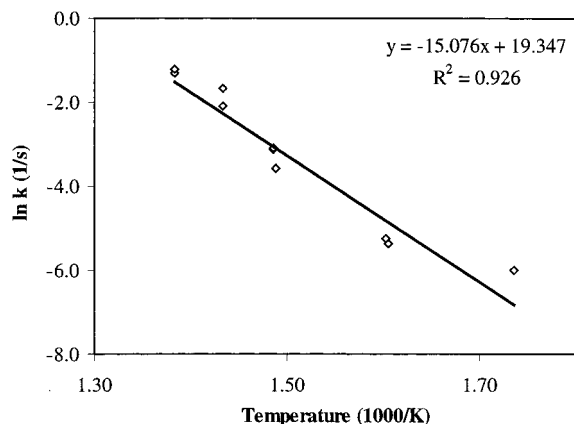
Figure 4. Arrhenius plot for hydrolysis of lactic acid (first-order model).

Table 3. First-Order Kinetic Parameters for Hydrolysis of Selected Carboxylic Acids

organic compd	A (1/s)	E_a (kJ/mol)	temp (°C)	pressure (MPa)	ref
lactic acid (TOC)	2.53×10^8	125	300–450	27.6	this work
acetic acid	2.51×10^4	94	475–600	24.6	25
formic acid	1.58×10^6	85.7	360–420	18–25	13

compounds such as methanol (409 kJ/mol)[7] and ethanol (340 kJ/mol).[41] It can be interpreted that the larger the activation energy, the more sensitive to temperature changes the reaction rate becomes. As shown in Table 1, the rate of lactic acid oxidation was slow at 315 °C and became extremely fast at 350 °C. Also, as is the case for methanol and ethanol, the pre-exponential factor for lactic acid is much higher as compared to that of acetic acid, resulting in a much faster rate. For example, the rate of lactic acid oxidation is about 3 orders of magnitude faster than that of acetic acid under similar conditions.

A relatively low activation energy (68.4 ± 27.2 kJ/mol) was obtained for the TOC kinetic model. Since TOC, a lumped parameter accounting for carbons from reactants and reaction intermediates including those refractory compounds such as acetic acid, the change in the overall rate of TOC reduction becomes less temperature-dependent. These refractory intermediates also increase the influence of oxygen in the reaction kinetics, as indicated by a larger n value (0.36) as compared to that for the lactic acid kinetic model ($n = 0.16$). Because of this strong dependency on oxygen concentration, a pseudo-first-order model cannot represent the experimental TOC conversion data well.

In addition, hydrolysis experiments were conducted to study the thermal stability of lactic acid at temperatures ranging from 300 to 450 °C. As shown in Figure 4, the TOC conversion for lactic acid hydrolysis displays a first-order reaction kinetics behavior. First-order reaction kinetic parameters for the hydrolysis of selected carboxylic acids are summarized in Table 3.

In summary, the best-fit model for LA oxidation and the best-fit TOC model, respectively, with 95% confidence limits are

$$-d[LA]/dt = 10^{18.7 \pm 4.2} \exp(-226 \pm 46.6 \text{ kJ/mol}/RT)[LA]^{0.88 \pm 0.11}[O_2]^{0.16 \pm 0.19}$$

and

$$-d[TOC]/dt = 10^{4.3 \pm 2.5} \exp(-68.4 \pm 27.2 \text{ kJ/mol}/RT)[TOC]^{0.62 \pm 0.33}[O_2]^{0.36 \pm 0.26}$$

Similarly, the best-fit TOC model for lactic acid hydrolysis is

$$-d[TOC]/dt = 10^{8.4 \pm 2.1} \exp(-125 \pm 26.7 \text{ kJ/mol}/RT)[TOC]$$

Reaction Pathways. In addition to the liquid and gaseous products derived from the HTO of lactic acid (Table 1), a more complex product matrix was generated from the lactic acid hydrolysis. Formic acid, acetic acid, propionic acid, acrylic acid, and acetaldehyde were found in the liquid effluent derived from lactic acid hydrolysis. Among gaseous products, hydrogen, carbon dioxide, carbon monoxide, and methane were quantified. Since no nitrogen species were involved in the reaction system, the nitrogen found in the gaseous effluent samples was believed to be the result of air contamination during sample handling. On the basis of these data, pathways involving hydrothermal reactions of lactic acid are proposed.

As shown in Figure 5, the decomposition of lactic acid in high-temperature water may follow three major pathways: hydrolysis/thermal degradation, dehydration, and oxidation. When an oxidant is present, the route leading to the formation of acetic acid predominates. This route begins with the hydrogen abstraction step followed by hydroxylation to form acetic acid and formic acid. Further decomposition of acetic acid follows the methane oxidation route producing carbon monoxide and eventually carbon dioxide. However, this step requires relatively high activation energy. As a result, acetic acid is a major and stable HTO reaction intermediate.[20] Similar results were found in the study involving the oxidation of propionic and butyric acids in supercritical water.[27] On the contrary, formic acid decomposes readily even under subcritical water conditions. The decomposition of formic acid follows both the dehydration route (producing CO and H_2O) and the decarboxylation route (producing CO_2 and H_2). Carbon monoxide can be further converted via the water–gas-shift (WGS) reaction.[43] The presence of the water–gas-shift reaction in HTO systems is supported by the fact that trace amounts of hydrogen were found in the effluent derived from the HTO of organic compounds.[25] However, equilibrium for the WGS reaction may not be reached under typical test conditions for kinetic studies.

As shown in Figure 6, both CO_2 and CO concentrations in the gaseous effluent increase with temperature, confirming that CO is relatively stable. Similar trends exist for formic acid decomposition in which the concentration of CO reaches to about 10 vol % at temperatures above 400 °C.[13,28] The concentration of CO can be as high as that of CO_2 (about 30 vol %) in the thermal decomposition of oxalic acid at temperatures ranging from 425 to 475 °C.[28]

Thermal degradation, hydrolysis, and/or dehydration of lactic acid in high-temperature water may occur simultaneously with or without oxygen. Without the presence of oxygen, acetaldehyde was found to be a major intermediate, suggesting that hydrolysis and/or thermal decomposition of lactic acid may involve an acetaldehyde precursor, such as pyruvic acid, and acetaldehyde was relatively stable in high-temperature water without the presence of an oxidant. The formation
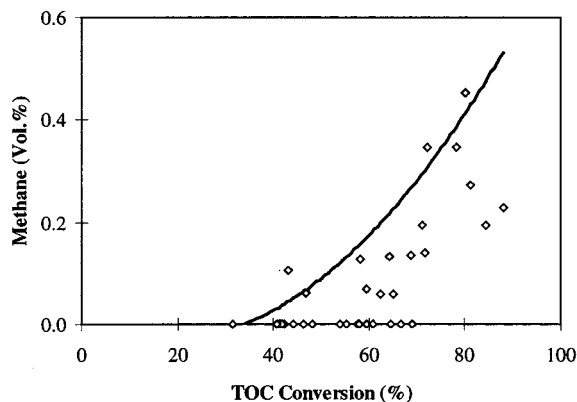
Note:
( ) — compounds identified by this work;
[ ] — compounds identified by this work, and references 10 and 34;
{ } — compounds identified by this work, and references 10, 25, and 34;
* — compounds identified by references 10 and 34;
** — compounds identified by references 10 and 25;
Dashed arrows — oxidative steps initiated by hydrogen abstraction at the α-carbon.

Figure 5. Proposed hydrothermal reaction pathways for lactic acid.

Figure 6. Formation of CO_2 and CO as a function of temperature in HTO of lactic acid.

Figure 7. CO concentration trend as a function of TOC conversion in HTO of lactic acid.

of acrylic acid and propionic acid in relatively high concentrations support the lactic acid dehydration pathway. Such a reaction can happen in high-temperature water with relatively high yields based on several studies involving the dehydration of ethanol[11] and *tert*-butyl alcohol[44] in supercritical water. Furthermore, small amounts of glycolic acid were found in a few

samples. Glycolic acid may be derived from 3-hydroxy-propionic acid via hydrogen abstraction at the α-carbon.

As an overall indicator, the amounts of all gaseous products, such as CO_2, CO, and CH_4, can be correlated with TOC conversion of lactic acid. As shown in Figures 7 and 8, the concentrations of CO and CH_4, respectively,

Figure 8. CH$_4$ concentration trend as a function of TOC conversion in HTO of lactic acid.

display consistent and increasing trends with TOC conversion.

Conclusion

Global kinetic models were developed for hydrothermal oxidation and hydrolysis of lactic acid at temperatures ranging from 300 to 400 °C and a pressure of 27.6 MPa. The rate of lactic acid oxidation showed a strong dependency on temperature under the test conditions, as indicated by the high activation energy (226 kJ/mol). However, as a result of forming stable reaction intermediates, the rate of TOC conversion was a weak function of temperature (i.e., activation energy = 68.4 kJ/mol), but a strong function of oxidant concentration. Hydrolysis of lactic acid proceeded concurrently under the test conditions. In this case, the TOC conversion followed a first-order reaction kinetics.

Acetaldehyde, acrylic acid, propionic acid, and to a lesser extent, acetic acid were identified as reaction intermediates for the hydrolysis of lactic acid. These results in combination with literature data provided a basis for the proposed pathways for hydrothermal reactions involving lactic acid. The results from this study demonstrated the possibility of converting lactic acid into various products in high-temperature water.

Acknowledgment

Literature Cited

(1) Modell, M. Gasification and Liquefaction of Forest Products in Supercritical Water. In *Fundamentals of Thermochemical Biomass Conversion*; Overend, R. P., Milne, T. A., Mudge, L. K., Ed.; Elsevier Applied Science Publ.: New York, 1985; Chapter 6.

(2) Xu, X.; Matsumura, Y.; Stenberg, J.; Antal, M. J., Jr. Catalytic Gasification of Biomass and Destruction of Waste Materials in Supercritical Water. *Ind. Eng. Chem. Res.* **1996**, *35* (8), 2522.

(3) Klein, M. T.; Torry, L. A.; Wu, B. C.; Townsend, S. H.; Paspeck, S. C. Hydrolysis in Supercritical Water: Solvent Effects as a Probe of the Reaction Mechanism. *J. Supercrit. Fluids* **1990**, *3* (4), 222.

(4) Sasaki, M.; Kabyemela, B.; Malaluan, R.; Hirose, S.; Takeda, N.; Adschiri, T.; Arai, K. Cellulose Hydrolysis in Subcritical and Supercritical Water. *J. Supercrit. Fluids* **1998**, *13*, 261.

(5) Modell, M. Supercritical Water Oxidation. In *Standard Handbook of Hazardous Waste Treatment and Disposal*; Freeman, H. M., Ed.; McGraw-Hill: New York, 1989; Chapter 8.

(6) Shaw, R. W.; Brill, T. B.; Eckert, C. A.; Franck, E. U. Supercritical Water—A Medium for Chemistry. *Chem. Eng. News* **1991**, Dec., 26.

(7) Tester, J. W.; Holgate, H. R.; Armellini, F. J.; Webley, P. A.; Killilea, W. R.; Hong G. T.; Barner, H. E. Supercritical Water Oxidation Technology: A Review of Process Development and Fundamental Research. In *Emerging Technologies for Hazardous Waste Management III*; Tedder, D. W., Pohland, F. G., Eds.; ACS Symposium Series 518; American Chemical Society: Washington, DC, 1992; Chapter 3.

(8) Gloyna, E. F.; Li, L. Supercritical Water Oxidation: An Engineering Update. *Waste Management* **1993**, *13* (5–7), 379.

(9) Savage, P. E.; Gopalan, S.; Mizan T. I.; Martino, C. J.; Brock. E. E. Reactions at Supercritical Conditions: Applications and Fundamentals. *AIChE J.* **1995**, *41* (7), 1723.

(10) Mok, W. S.-L.; Antal, M. J. Formation of Acrylic Acid from Lactic Acid in Supercritical Water. *J. Org. Chem.* **1989**, *54* (19), 4596.

(11) Xu, X.; Almeida, C. D.; Antal, M. J., Jr. Mechanism and Kinetics of the Acid-Catalyzed Dehydration of Ethanol in Supercritical Water. *J. Supercrit. Fluids* **1990**, *3* (4), 228.

(12) Bjerre, A. B.; Sorensen, E. Thermal Decomposition of Dilute Aqueous Formic Acid Solutions. *Ind. Eng. Chem. Res.* **1992**, *31* (6), 1574.

(13) Yu, J.; Savage, P. E. Decomposition of Formic Acid under Hydrothermal Conditions. *Ind. Eng. Chem. Res.* **1998**, *37* (1), 2.

(14) Gupta, R.; Johnston, K. P. Ion Hydration in Supercritical Water. *Ind. Eng. Chem. Res.* **1994**, *33*, 2819.

(15) Xiang, T.; Johnston, K. P. Acid—Base Behavior of Organic Compounds in Supercritical Water. *J. Phys. Chem.* **1994**, *98* (32), 7915.

(16) Mishra, V. S.; Mahajani, V. V.; Joshi, J. B. Wet Air Oxidation. *Ind. Eng. Chem. Res.* **1995**, *34* (1), 2.

(17) Gloyna, E. F.; Li, L. Supercritical Water Oxidation for Remediation of Wastewaters and Sludges. in *Encyclopedia of Environmental Analysis and Remediation*; Meyers, R. A., Ed.; John Wiley & Sons: New York, 1998.

(18) Vallejo, D. F. Synthesis of Acetic Acid from Nontraditional Feedstocks in Subcritical and Supercritical Water Oxidation. M.S. Thesis, Civil Engineering Department, The University of Texas at Austin, Austin, TX, 1996.

(19) Li, L.; Gloyna, E. F. Separation of Ionic Species under Supercritical Water Conditions. Presented at the Tenth Symposium on Separation Science and Technology for Energy Applications, Gatlinburg, TN, Oct 20–24, 1997.

(20) Li, L.; Chen, P.; Gloyna, E. F. Generalized Kinetic Model for Wet Oxidation of Organic Compounds. *AIChE J.* **1991**, *37* (11), 1687–1697.

(21) Ding, Z. Y.; Frisch, M. A.; Li, L.; Gloyna, E. F. Catalytic Oxidation in Supercritical Water. *Ind. Eng. Chem. Res.* **1996**, *35* (10), 3257.

(22) Lee, D. S. Supercritical Water Oxidation of Acetamide and Acetic Acid. Ph.D. Dissertation, Civil Engineering Department, The University of Texas at Austin, Austin, TX, 1990.

(23) Rice, S. F.; Steeper, R. R.; LaJeunesse, C. A. *Destruction of Representative Navy Wastes Using Supercritical Water Oxidation*; Sandia Report SAND94-8203·UC-402, Sandia National Laboratories: Livermore, CA, 1993.

(24) Li, L.; Chen, P.; Gloyna, E. F. Pilot-Plant Validation of Global Kinetic Models for Supercritical Water Oxidation. In *Chemical Oxidation: Technology for the Nineties*; Eckenfelder, W. W., Bowers, A. F., Roth, J. A., Eds.; Technomic Publishing Co.: Lancaster, PA, 1997; Vol. 4, p 219.

(25) Meyer, J. C.; Marrone, P. A.; Tester, J. W. Acetic Acid Oxidation and Hydrolysis in Supercritical Water. *AIChE J.* **1995**, *41* (9), 2108.

(26) Foussard, J.; Debellefontaine, H.; Besombes-Vailhe, J. Efficient Elimination of Organic Liquid Wastes: Wet Air Oxidation. *J. Environ. Eng.* **1989**, *115* (2), 367.

(27) Wilmanns, E. G. Supercritical Water Oxidation of Volatile Acids. M.S. Thesis, Civil Engineering Department, The University of Texas at Austin, Austin, TX, 1990.

(28) Crain, N. E. Supercritical Water Oxidaiotn Kinetics of Propellant Simulant. Ph.D. Dissertation, Civil Engineering Department, The University of Texas at Austin, Austin, TX, 1994.

(29) Baillod, C. R.; Faith, B. M.; Masi, O.; Fate of Specific Pollutants During Wet Oxidation and Ozonation. *Environ. Progress* **1982**, *1* (3), 217.

(30) Wightman, T. J. Studies in Supercritical Wet Air Oxidation. M.S. Thesis, University of California at Berkeley, Berkeley, CA, 1981.

(31) Shende, R. V.; Mahajani, V. V. Kinetics of Wet Oxidation of Formic Acid and Acetic Acid. *Ind. Eng. Chem. Res.* **1997**, *36* (11), 4809.

(32) Shende, R. V.; Mahajani, V. V. Kinetics of Wet Air Oxidation of Glyoxalic Acid and Oxalic Acid. *Ind. Eng. Chem. Res.* **1994**, *33* (12), 3125.

(33) Datta, R.; Tsai, S. P. Lactic-Acid Production and Potential Uses: A Technology and Economics Assessment. *ACS Symp. Ser.* **1997**, *666*, 224.

(34) Lira, C. T.; McCrackin, P. J. Conversion of Lactic Acid to Acrylic Acid in Near-Critical Water. *Ind. Eng. Chem. Res.* **1993**, *32* (11), 2608.

(35) Gunter, G. C.; Craciun, R.; Tam, M. S.; Jackson, J. E.; Miller, D. J. FTIR and P-31-NMR Spectroscopic Analysis of Surface Species in Phosphate-Catalyzed Lactic-Acid Conversion. *J. Catal.* **1996**, *164* (1), 207.

(36) Tam, M. S.; Gunter, G. C.; Craciun, R.; Miller, D. J.; Jackson, J. E. Reaction and Spectroscopic Studies of Sodium-Salt Catalysts for Lactic-Acid Conversion. *Ind. Eng. Chem. Res.* **1997**, *36* (9) 3505.

(37) Croiset, E.; Rice, S F.; Hanush, R. G Hydrogen-peroxide Decomposition in Supercritical Water. *AIChE J.* **1997**, *43* (9), 2343.

(38) Croiset, E.; Rice, S F. Direct Observation of H_2O_2 during Alcohol Oxidation by O_2 in Supercritical Water. *Ind. Eng. Chem. Res.* **1998**, *37* (5) 1755.

(39) Bourhis, A. L.; Swallow, K. C., Hong, G. T.; Killilea, W. R. The Use of Rate Enhancers in Supercritical Water Oxidation. In *Innovations in Supercritical Fluids Science and Technology*; Hutchenson, K. W., Foster, N. R., Eds.; ACS Symposium Series; American Chemical Society: Washington, DC, 1995; Vol. 508, p 338.

(40) Cutler, A. H.; Antal, M. J., Jr.; Jones, M., Jr. A Critical Evaluation of the Plug-Flow Idealization of Tubular-Flow Reactor Data. *Ind. Eng. Chem. Res.* **1988**, 27, 691.

(41) Helling, R. K. Oxidation of Simple Compounds and Mixtures in Supercritical Water: Carbon Monoxide, Ammonia and Ethanol. Ph.D. Dissertation, MIT, Cambridge, MA, 1986.

(42) Foussard, J. Study on Aqueous Phase Oxidation at Elevated Temperatures and Pressures. Ph.D. Dissertation, National Institute of Applied Science, Toulouse, France, 1983.

(43) Holgate, H. R.; Webley, P. A.; Tester, J. W.; Helling, R. K. Carbon Monoxide Oxidation in Supercritical Water: The Effects of Heat Transfer and the Water−Gas Shift Reaction on Observed Kinetics. *Energy Fuels* **1993**, *6* (5), 586.

(44) Xu, X.; Antal, M. J., Jr. Mechanism and Kinetics of the Auto-Catalytic Dehydration of t-Butanol in Near-Critical Water. Presented at AIChE Annual Meeting, Los Angeles, CA, Nov 17−22, 1991.